Salting-Out Effect Induced by Temperature Cycling on a Water/Nonionic Surfactant/Oil System

Nicolas Anton,[†] Patrick Saulnier,*[,†] Arnaud Béduneau,[†] and Jean-Pierre Benoit[†,‡]

Inserm U646, Ingénierie de la vectorisation particulaire, Université d'Angers, F-49100 Angers, France, and École pratique des hautes études (EPHE), 12 rue Cuvier, F-75005 Paris, France

Received: October 2, 2006; In Final Form: February 2, 2007

This paper presents original effects induced by temperature cycling on the transitional phase inversion of emulsions, stabilized by a nonionic polyethoxylated C18E6 surfactant model. The phase inversion follow-up is performed by electrical conductivity measurements, which involves focusing the study on the shape and location of the emulsion inversion region. In that way, new observations are brought out as a gradual evolution of the emulsion inversion along the cycling process. Two alternative approaches are considered for tackling these results: (i) first, a molecular approach regarding the particular organization and rearrangement of water clusters surrounding the surfactant polymer polar head, and (ii) second, a thermodynamic approach only considering the whole Gibbs free energy of the system. The volumic approaches are transposed, here, to the water/oil interface, and disclose that the phase inversion zone is included in a metastable region, able to stabilize for a given temperature, either metastable O/W emulsions or stable W/O ones. In that way, this study proposes novel and complementary insights into the phenomena governing the emulsion phase inversion.

Introduction

Aqueous solutions of nonionic surfactants such as polyethylene oxide monoalkyl ether, C_xE_y, form a large range of structures and mesophases widely investigated in the literature. Many works[1−8] elucidate this phase behavior as the consequence of the hydration state of the surfactant ethylene oxide (EO) chains. More precisely, the self-association and water solubility of nonionic surfactant are totally governed by water molecules' structure, associated by hydrogen bonds into flickering clusters, and wrapping the polar head. In addition, above a particular temperature, the so-called cloud point (CP), the surfactant becomes insoluble as a consequence of poor interactions between the EO head and the bulk. Then a demixing occurs and the two forming phases are a surfactant-rich phase and an aqueous phase at a surfactant concentration near the critical micelle concentration (cmc). Faced with the large number of phase behaviors and structures involved in the use of nonionic surfactant, the study of the solubility state of such a molecule is commonly performed with the CP determination. The CP reflects the hydration state of the OE heads, and therefore the median cluster size (average number of water molecules in the flickering clusters). Numerous studies have been focused on the effects of formulation parameters and additives, which induce changes in cmc[9−19] or in CP,[11,14,20−31] so acting on the structure of the water cluster and modifying the following equilibrium.

$$n\mathrm{H_2O} \leftrightarrows (\mathrm{H_2O})_n$$

In fact, such an equilibrium is affected by the temperature and the surfactant concentration (in particular conditions[32]), but mostly by the electrolyte concentration in water which induces salting-in or salting-out effects,[11,20,24,33−37] shifting the above equilibrium toward the left or the right, respectively. Each one of these effects is algebraically additive, as is the competition between the ones induced by anions and cations. As a result, the higher the level of association of water into clusters (high median cluster size), the lower the solubility of the polar OE heads, and vice versa.

To clarify the role of such a cluster on the nonionic surfactant solubility, it is important to present at this point the main approaches proposed to explain the apparent solubility, and more exactly the interaction of the water (from the bulk) with EO chains.[38−43] A first approach is based on the ability of the ethylene oxide group to create hydrogen bonds with the bulk water,[38,39] making the polymer intimately linked to the bulk and thereby increasing its solubility. Another approach consists of considering that the conformation of the EO unit may induce a localized dipole moment (larger in the cis conformation), which creates molecular interactions with the polar water molecules of the bulk.[40,41] Only these two approaches will be taken into account in this paper, even if the literature provides more models.[42,43] Now, the influence of the water flickering clusters on this interaction is easily imaginable, as a buffer or shielding effect, which increases with a rise in the level of the water molecules' structure. Furthermore, two competitive effects occur with the rise of the temperature: (i) The first one, previously mentioned, leads to breakup of the water structure; the literature provides[44,45] for pure water, with the median cluster size as a decreasing function of the temperature. (ii) The second one, involved by the existence of the cloud point, leads to lower solubility as a consequence of the excitation of water bulk molecules, which decreases their interactions with the ethylene oxide. Of course, (ii) wins this competition.

On the other hand, a second approach for tackling these phenomena is also conceivable, as rather a global thermodynamic approach. Indeed, instead of considering the surfactant behavior as a result of the intermolecular rearrangements of

* To whom correspondence should be addressed. Telephone: + 33 241 735 855. Fax: + 33 241 735 853. E-mail: patrick.saulnier@univ-angers.fr.
[†] Inserm U646, University of Angers.
[‡] EPHE.

10.1021/jp0664768 CCC: $37.00
Published on Web 03/17/2007

water molecules, a different and thermodynamic way can also be considered, focusing the study on the global Gibbs free energy of water/nonionic surfactant systems. This approach was reported in recent works of Hołyst et al.,[46−48] in which homogeneous mixtures (uniform states, below the CP) and two-phase systems (above the CP) are described through a single minimum of Gibbs free energy. These authors revealed the presence of hidden minima of free energy in the transitional region between the two single-minimum states, the so-called metastable region.[46] Then, according to the thermal and kinetic pathways imposed on the system, for a given temperature in the metastable region, it is possible to observe either a metastable homogeneous system or a stable phase-separated system.

Water solubility of nonionic surfactant, investigations on the cloud point, and investigations on the phase inversion temperature (PIT) of water/nonionic surfactant/oil system are closely related phenomena.[49,50] We study in the present paper the surfactant behavior, this time at the water/oil interface, within a ternary {water/nonionic surfactant/oil} system. Therefore, the two approaches presented above are transposed to the interface in order to originally tackle the emulsion phase inversion and the influence of the thermal and kinetic pathways on the surfactant behavior when stabilizing the emulsion. We have focused the experimental studies on the phase inversion temperatures as well as on the size of the transitional zone between the O/W and W/O macroemulsions, assumed to exhibit bicontinuous microemulsion structures.[51−53] In addition to the common works on the PIT location, emulsion characterization within the inversion zone, or even the phase diagram determination of such a system,[51−53] the purpose of this study is to investigate the original role of the temperature cycles performed around the emulsion inversion (as a particular pathway). Surprising effects induced by temperature cycling of the emulsion are reported, and hypotheses on the physicochemical behavior of nonionic surfactant molecules are proposed. The characterizations are performed by conductivity measurements. Likewise, a few reported[54−59] formulations of nanoparticles and nanocapsules which are prepared following phase-inversion-based processes include temperature cycling technology. Such a stage is not well understood, and our aim here is also to clarify this aspect.

Experimental Section

Materials. A polyethylene oxide monoalkyl ether model surfactant, C18E6, kindly furnished by Stearinerie-Dubois (Boulogne, France), was exclusively used in this study. A strong salting-out agent, sodium chloride, was obtained from Prolabo (Fontenay-sous-Bois, France). The oil used was a light mineral oil, a standardized denomination to refer to a mixture of saturated hydrocarbons obtained from petroleum; it was purchased from Cooper (Melun, France). Finally, Ultrapure water was obtained by a MilliQ filtration system (Millipore, Saint-Quentin-en-Yvelines, France).

Methods. The emulsion was constantly and mechanically stirred at around 900 rpm for all described experiments using an IKA Eurostar digital stirring motor (VWR, Fontenay-sous-Bois, France). The heating plate used was a Bioblock device (Illkirch, France).

Conductivity Measurements. A conductimeter (Cond 330i/SET, WTW, Germany) was used in nonlinear temperature compensation mode, according to EN 27 888. This allowed the determination of the location of the emulsion inversion following conductivity variation according to the temperature. In fact, a conductivity value lower than 10 $\mu S \cdot cm^{-1}$ and essentially zero

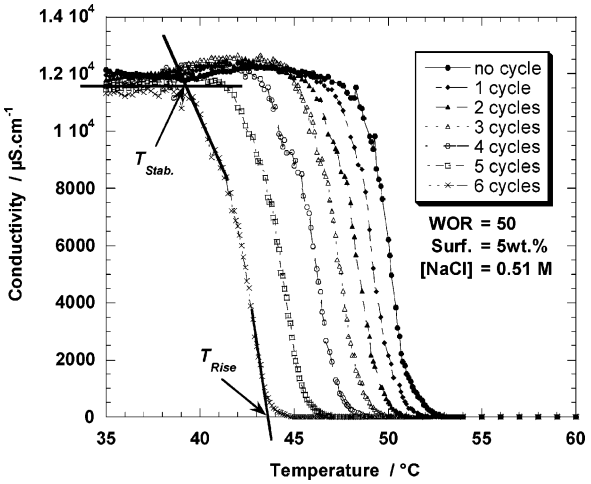

Figure 1. Experimental values of conductivity against temperature showing the emulsion phase inversion. The studied system is {WOR = 50; surfactant wt % = 5; [NaCl] = 0.51 M}. The measures are reported for six cycles of temperature; the curves show a shift to the left with the cycling.

on the illustrated scales means that the continuous phase is oil, whereas a high steady state reached reflects that a water continuous phase is established. The transitional region shows a continuous variation of conductivity between the two emulsion types (W/O and O/W); this has been attributed to bicontinuous microemulsion structures.[51−53] The shape of such a transitional region, and its width and location in the temperature range, provides indications on the relative solubility state of the surfactant and relative hydration of the polymer chain, as it is proposed and discussed in this paper.

Furthermore, in order to compare the influence of the composition and formulation variables, as well as the effect of temperature cycling, on the shape, particular landmarks were chosen in each conductivity curve: (i) the temperature of the first conductivity rise during the cooling of the W/O emulsion, called T_{Rise}, and (ii) the temperature of the conductivity stabilization in the O/W emulsion state, $T_{Stab.}$, just after the passage through the bicontinuous region (during the cooling process as well). In that way, this paper will present the follow-up of the location of the emulsion inversion with T_{Rise}, and of the bicontinuous microemulsion zone width with $\Delta T_{\mu e} = T_{Stab.} - T_{Rise}$. Additional indications on T_{Rise} and $T_{Stab.}$ determination on the conductivity vs temperature curves will be provided on the first results in Figure 1.

In all experiments, we have studied the ternary system {aqueous phase; surfactant; mineral oil}, where the "aqueous phase" is defined as "water plus electrolyte". The formulation variable was chosen as the electrolyte concentration, and the composition ones were defined as surfactant weight percentage, surf. wt %, and as the water−oil ratio, WOR, which is the (100 × water/(water + oil)) weight ratio.

Temperature Cycling. Temperature cycles, denoted "T-cycles", were performed around the PIT, and more precisely within the fixed temperature window 35 °C < T < 60 °C, following a given and fixed rate: $\partial T/\partial t = \pm 1.5$ °C/min. The two choices and their influences on the results are discussed below. As a last remark, all conductivity measurements performed in this work were done in the case of $\partial T/\partial t < 0$; since the results for $\partial T/\partial t > 0$ are nearly the same when we compare the curves framing a minimum of temperature, they are not shown. Oil and water plus electrolyte were mixed, and the amphiphile was gradually added during the first heating under constant stirring. The system was raised to the fixed upper limit

60 °C to homogenize it, and then the first measures began with the cooling. This first curve was considered the starting point of the temperature cycling, i.e., noted as "no cycle". The experiments were performed three times.

Results and Discussion

Conductivity vs Temperature Curves: An Illustration. An isolated conductivity curve presents its expected shape, and the two plateaus indicate the macroemulsions locations.[50,60−62] The new observation is that a process of cycling of temperature around the phase inversion zone can induce a modification of such a curve, either (i) a global shift of the curve in the studied temperatures range, or (ii) the enlarging of the transitional bicontinuous region, or both (i) and (ii) can occur simultaneously, or even more not occur at all.

These four different cases are observed for identical, given, temperature treatment. The selection only depends on the composition and formulation variables. In concrete terms, the effects (i) and (ii) result in the change of T_{Rise} and $\Delta T_{\mu e}$, respectively. Case (i), as an illustration, is provided in Figure 1. The complete study will be developed below and will disclose the role of the so-called composition and formulation parameters on these two effects.

We have defined the particular temperatures T_{Rise} and $T_{\mathrm{Stab.}}$ (indicated, for instance, in the last curve in Figure 1), as the intersection between the straight line that fits the transitional conductivity variation and the stabilized conductivity. The curves report the conductivity as a function of temperature, all along the T-cycles, and for the same sample. The trends appear here as a decrease of the T_{Rise} with the temperature cycling. The complete study of all cases discloses a similar decreasing behavior (in the cases, of course, where T_{Rise} does not remain constant). Also, in Figure 1 the stabilization of the conductivity value (O/W emulsion) is nearly the same for all the curves, around 12 mS·cm^{-1}; nevertheless, it did not remain relevant in the context of this study, since it focused the interest on the examination of the global shape of the curves to characterize the emulsion phase inversion.

Formulation/Composition Scan without Temperature Cycling. First, in order to identify precisely the role of the T-cycling, we will first study, without temperature cycling, the location of the dynamic emulsion inversion as a function of the formulation and composition parameters. T_{Rise} and $T_{\mathrm{Stab.}}$ locations are reported below, as a function of [NaCl] in Figure 2a, and of the WOR in Figure 2b. The transitional conductivity zone is represented as a vertical line connecting T_{Rise} and $T_{\mathrm{Stab.}}$, and above and below these limits, the system shows W/O and O/W emulsions, respectively. Representative cases were chosen, WOR = 40 for Figure 2a and [NaCl] = 0.51 M for Figure 2b, and the surfactant amount equal to 5 and 10 wt % in the two cases. It should be noted that a change of the parameters does not actually change the global shape of the curves.

The global influence of the electrolyte concentration increase, Figure 2a, appears as a decrease of T_{Rise}, here about 10 °C between 0.03 and 0.75 M, whatever the studied surfactant contents. However, the width of the transitional microemulsion region remains virtually unchanged with the electrolyte concentration. Finally, the surfactant amount in the mixtures also has a role in the location of the emulsion inversion temperature about 12 °C between 5 and 10 surfactant wt %. Such an effect of the surfactant amount has been explained as the result of a fractionation process,[63] mainly due to the fact that the polyethoxylated surfactant may be a mixture of different oligomers, which is true in most cases.

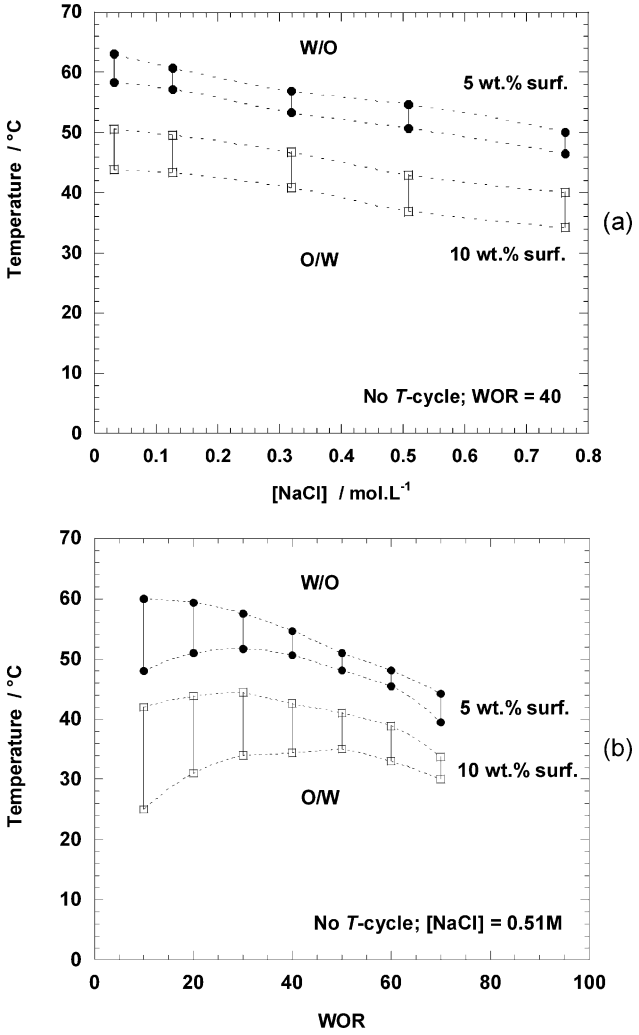

Figure 2. Experimental values summarized from the conductivity vs temperature curves without T-cycle. See the text for explanations. (a) Influence of the electrolyte concentration, for 5 and 10 surfactant wt %, at fixed WOR = 40. (b) Influence of the WOR, for 5 and 10 surfactant wt %, at fixed [NaCl] = 0.51 M.

The effects induced by the electrolyte are strongly dependent on its nature, and sodium chloride mainly used in this study was chosen for its nature to salt nonelectrolyte out. The trends of the curves in Figure 2a are well consistent with this fact (as are all the not shown curves with different WORs or different surfactant amounts), and somewhat confirm the correlations made between the cloud point and the PIT. Effects of the salting-out electrolytes are well-described in the literature,[2,37,64] and are due to strong electric fields created by the salts in the bulk. As a consequence, the structure of the water layer wrapping and hydrating the polymer chain is enhanced and the median cluster size increased. Such a phenomenon induces an entropy loss and leads to a steady state: The solubility of the polyethoxylated surfactant is definitely lowered.

In the case of the nonionic surfactant at the water/oil interface under stirring, and according to Bancroft's rule, its difference in solubility between both phases governs the interface curvature and hence determines the continuous phase. The location of the phase inversion zone reflects such a behavior of the surfactant, and the correlation PIT/cloud point presented indicates that the emulsion inversion process is mainly driven by the "nonionic surfactant/bulk water" interactions.

Nevertheless, it should be noted that emulsion on the one hand and surfactant in pure water on the other hand involve

relatively different amphiphile behaviors. Hence, isolated values of PIT and CP for the same system cannot be compared, as opposed to as the parallel drawn between their global behavior with changes of the composition and formulation variables. Explanations are provided by the interdependence of PIT and the nature of the oil; the surfactant migrates from and to the interface with the temperature, inducing a change of the partitioning coefficient.[65,66] Besides, their behaviors with the modification of electrolyte concentration remain widely similar.[49,50]

On the other hand, Figure 2b shows the emulsion phase inversion as a function of the WOR, at fixed electrolyte concentration [NaCl] = 0.51 M. Regarding this figure, obvious conclusions are not allowed, since the total amount of electrolyte also grows with the WOR. That comes from the fact that electrolyte concentration was maintained constant in the aqueous phase whatever the WOR. However, this choice is very important in the whole study to keep constant the apparent (and local) electrolyte concentration per surfactant molecule at the interface. We can stress the fact that the ternary system we have chosen in this paper is {salt water; oil; surfactant}.

Figure 2b shows the emulsion inversion in a large range of WORs, between 10 and 80, which induces remarkable differences in $\Delta T_{\mu e}$, e.g., $\Delta T_{\mu e} \approx 19$ °C for WOR = 10 and $\Delta T_{\mu e} \approx 5$ °C for WOR = 80. The literature reports[51−53] this transitional region between the O/W and W/O macroemulsions exhibiting bicontinuous structures, microemulsion-like and nanoscaled. Regarding now the lipophilic nature of the model surfactant we used here, it essentially remains in the oily phase. Thus the transitional bicontinuous systems appear as water-in-oil microemulsions. Therefore, the lower the WOR, the higher the solubilization of water within the oily microemulsion. The fineness of the microemulsion network is assumed to be enhanced for low WOR, as well as the surfactant concentration at the water/oil interface. Hence, we propose the following idea, that the size of the bicontinuous region, $\Delta T_{\mu e}$, and the surfactant concentration at water/oil interface are linked. The microemulsion remains stabler as the surfactant interfacial concentration increases, and a larger transitional microemulsion zone is held as a result. In particular cases, the temperature cycling of the emulsion induces a rise of $\Delta T_{\mu e}$ which increases with the number of T-cycles; it is assumed to be a consequence of the rise of the surfactant interfacial concentration (developed within the following sections).

Over the left and right limits on Figure 2b, say for approximately WOR > 80 and WOR < 10, the emulsion inversion does not occur, due to oil or water excessively rich regions. The formulation vs composition maps commonly reported in the literature[51] present all the same from these frontiers, a morphology change with the temperature between the "normal" and "abnormal" emulsion types, in agreement with Brancoft's rule or not, respectively. The rest of the study will deal with the effects of the temperature cycling in a intermediate range of WOR (mainly WOR = 40, 50, 60) in order to reduce the initial WOR effects, and only to consider the T-cycling effects.

Effects of Temperature Cycling on Emulsion Phase Inversion: Effects on T_{Rise}. Let us consider in the present part the follow-up along the T-cycling, of the temperatures T_{Rise}, at which the emulsion conductivity begins to increase during the W/O to O/W transition. The global effect (when it exists) induced by the temperature cycles is a shift of the conductivity curves to the lower temperatures, i.e., a drop of T_{Rise}. Such behavior appears surprising, novel, and original. The illustration is done with Figure 3 (and below in Figure 4), where the roles played by the electrolyte concentration and by the WOR on the trends of the curves were investigated.

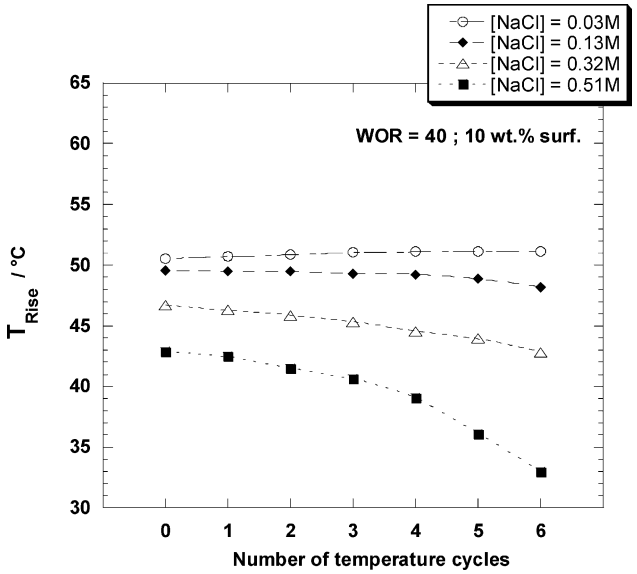

Figure 3. Experimental values of T_{Rise} with temperature cycling, presenting movement of the conductivity curves to lower temperatures. Influence of [NaCl] at fixed WOR = 40 and surfactant amount = 10 wt %.

The drop of T_{Rise} with the number of cycles is clearly induced by the quantity of electrolyte; in concrete terms, the variation of the curves after seven cycles is nearly zero for low NaCl concentrations and reaches about 10 °C for [NaCl] = 0.51 M. Such behavior indicates a loss in the surfactant affinities for the aqueous phase with an increase of the temperature, described as a loss in the intermolecular interactions PEO/bulk water due to the thermal excitation of the bulk. Here it is clear that temperature cycles enhance the salting-out effect, acting on the surfactant environment, the hydration structure surrounding the polymer. The emulsion phase inversion we observe in this study appears as its macroscopic expression.

The influences of the WOR and the surfactant amount on T_{Rise} were also investigated for representative cases, and are reported in Figure 4. The electrolyte concentration is here fixed at [NaCl] = 0.13 M in Figure 4a and 0.51 M in Figure 4b, and results are consistent with the behavior previously shown in Figure 3. The lower sodium chloride concentration in water presented with 0.13 M does not induce any shift in the conductivity curves with the temperature cycling, whereas it appears with 0.51 M. Furthermore, the effect is accentuated by the decrease of the water/oil ratio and also, but in lower orders of magnitude, by the decrease of the surfactant amount.

The first approach for discussing such phenomena is a molecular approach, which essentially regards the size and rearrangement of the flickering water clusters surrounding the surfactant polar heads. Since this water cluster network is assimilated to a barrier which reduces the interactions surfactant/bulk water, the size and density of this barrier are closely linked to the surfactant solubility in water, and thus to the location of the emulsion inversion (as T_{Rise}). The idea we propose here to explain the behavior disclosed in Figure 3 is based on the potential ability of the cluster network to increase its structuring, order, and density along the T-cycling process. On the one hand (as previously discussed), the median cluster size decreases when increasing the temperature and vice versa; then the heating/cooling process incessantly disturbs the cluster network.[44,45] Such fluctuations are so weak that this effect is still outweighed

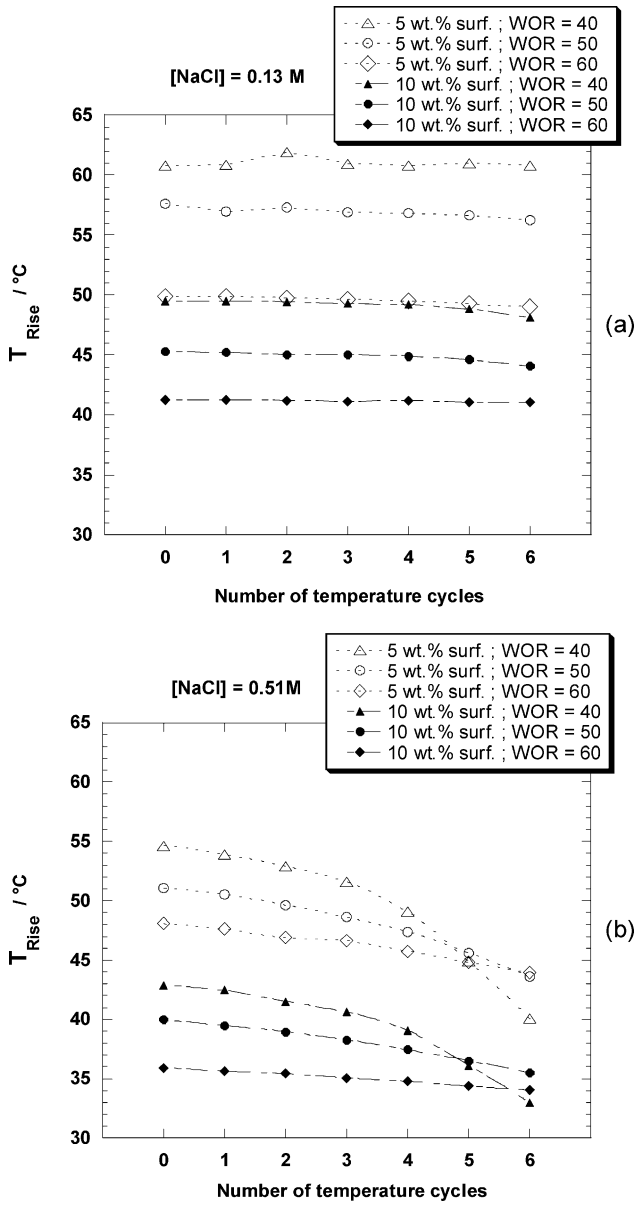

Figure 4. Experimental values of T_{Rise} with temperature cycling. Influence of the composition variables on the shift of the conductivity curves, at fixed [NaCl], 0.13 M in (a) and 0.51 M in (b). Surfactant amounts are equal to 5 wt % (open symbols) and to 10 wt % (filled symbols), with the WORs varying from 40 to 60.

by the loss of the surfactant solubility due to the water thermal excitation (inducing the phase inversion). However, the shift toward lower temperatures of the emulsion inversion zone suggests a gradual enhancing of the cluster network shielding effect, and thus a gradual increase of the water structure and density. Moreover, according to the influence of the NaCl concentration on this effect, the order induced by the presence of electrolyte in solution appears to contribute to the water structuring during the cycling. The electrolyte concentration gradient, between the bulk and nearby surrounding region of the PEO, intrinsically induces a latent ability to rearrange, revealed with the cycling process.

Let us move now to the second thermodynamic approach for tackling these phenomena. Such an aspect involves consideration of the Gibbs free energy of the ternary system as a whole, and then following its evolution on the profile of Gibbs free energy as a function of the arbitrary concentration of the water continuous phase.

Inspired by the volumic approach of Hołyst et al.,[46] the interfacial behavior of nonionic surfactant, here, can be described with Figure 5a. The two configurations that exhibit a single minimum of Gibbs energy are the so-called stable regions, for lower and higher temperatures, corresponding respectively to the stabilization of O/W and W/O macroemulsions. The thermodynamic equilibriums (at which the formation of emulsions is achieved) are attained at points A and B (for O/W and W/O emulsions, respectively). Between these two stable domains we can consider, as well, the existence of a metastable region, able for a given temperature to exhibit either a metastable O/W emulsion or a stable W/O one: This is precisely the origin of the evolution of T_{Rise}. In fact (still similarly to ref 46), for a given temperature in the metastable region, the energetic barrier divides the landscape (i) into the local basin stabilizing the O/W emulsion (where for example C_1 is the local minimum), and (ii) into the global (deepest) one forming the W/O emulsion (e.g., where C_3 is the global minimum). In that way, the thermal and kinetic pathways (such as the temperature cycling) imposed on the system totally govern the energetic state within the metastable region. In parallel, Figure 5b shows the schematic correlation between the thermodynamic aspect and the conductivity curves.

Since the slopes of the upper and lower stable regions are different, the cycling of temperature between them should induce a shift of the system Gibbs energy. Vertical dashed lines in Figure 5, S_1, S_2, and S_3, represent three given energetic states of the system. When the system state is, for instance, S_1, it is clear that in the metastable region the emulsion will exhibit the (metastable) O/W configuration. Also, for S_3, the emulsion is definitively trapped in the global minima of the metastable zone. In the intermediate states, e.g., S_2, a temperature change induces a crossing of the emulsion inversion within the metastable zone. The system typically stabilizes a W/O emulsion in C_2 and an O/W one in E, and exhibits an intermediate state at the phase inversion temperature in D (on the maximum of the activation energy barrier). Accordingly, the temperature cycling induces a shift of the phase inversion location from S_1 to S_3. This is precisely the reason why it is possible to observe simultaneously systems which exhibit the W/O and O/W emulsions, and both in the metastable region (e.g., for three cycles in Figure 1 modeled by the state S_2 in Figure 5). Finally, this interfacial approach clearly appears in a good coherence, not only with our experimental results, but also with the volumic approach of the literature.

It is also noteworthy that this observed salting-out effect induced by the T-cycles may completely disappear under different cycling conditions, for instance, when the temperature scanning window ΔT is reduced (e.g., for 15 °C fewer than the $\Delta T = 25$ °C defined for all the experiments in this paper). The rate of temperature variations $\partial T/\partial t$ is also a factor which can modify such a behavior. Data are not shown in the present study since only weak fluctuations are induced and the global trends remain unchanged; we rather chose to scan the formulation/composition variables. These remarks are likewise still in agreement with the two presented approaches. To finish, the effect of the electrolyte concentration which induces the emulsion inversion shift in Figure 3 appears, seen from that angle, intimately linked to the shape of the free energy within the metastable region and thus to its width. The local minimum even disappears in the case of very low NaCl concentration (e.g., 0.03 M).

Effects of Temperature Cycling on the Emulsion Phase Inversion: Effects on the Width of the Transitional Zone, $\Delta T_{\mu e}$. The last point of this study deals with the enlarging of

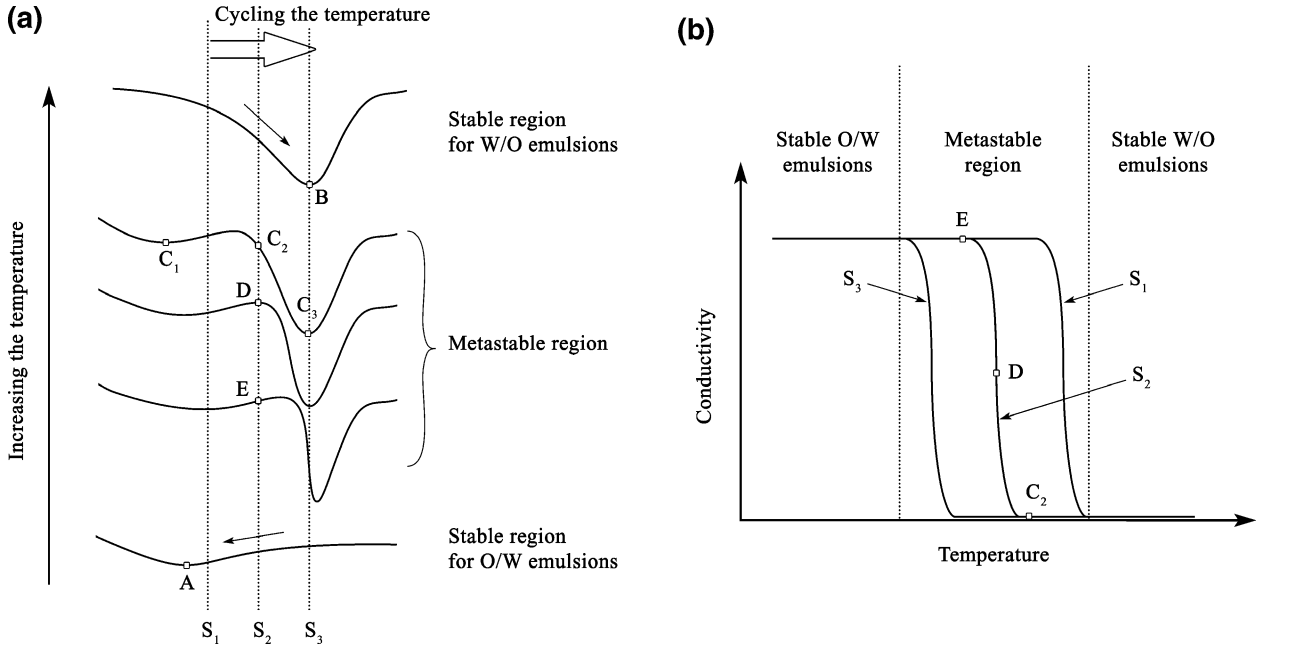

Figure 5. (a) Drawing representation of the Gibbs free energy as a function of the concentration of water continuous phase in the scanned range of temperature. Point A is the equilibrium state of the O/W emulsion formation; point B is the equilibrium state of the W/O one. The point C_1 shows the metastable state of the O/W emulsion stabilization, and C_3 shows the global minimum corresponding to the W/O stabilized emulsion (see a detailed description in the text). Three representative energetic states S_1, S_2, and S_3 are schematically represented, illustrating the gradual evolution of the emulsion inversion location. (b) A schematic representation of the emulsion inversion is correlated with the thermodynamic approach of (a), and illustrates the impact of the Gibbs free energy profile on the emulsion inversion shifting.

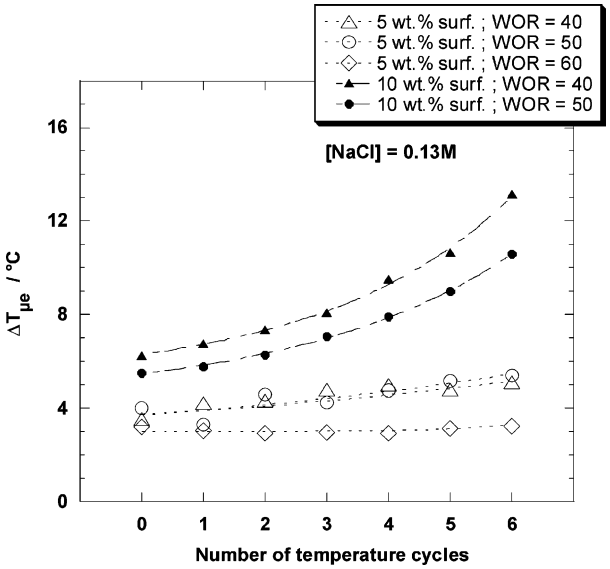

Figure 6. Experimental values of the width of the transitional conductivity region, $\Delta T_{\mu e} = T_{\text{Rise}} - T_{\text{Stab.}}$, and evolution during the temperature cycling. The presented systems show typical behaviors obtained relating the enlarging of the bicontinuous zone. The experiments are performed at fixed [NaCl] = 0.13 M, and studying the influence of WOR and surfactant amount.

the microemulsion zone, $\Delta T_{\mu e} = T_{\text{Rise}} - T_{\text{Stab.}}$, also induced by the cycling of temperature. This aspect is rather dissociated from the salting-out effect that may indicate different origins. Indeed, Figure 6 presents the evolution of $\Delta T_{\mu e}$ for selected representative cases.

The trends are divided into a gradual increase of $\Delta T_{\mu e}$ and a relative stability, e.g., variations around 7 and 1.5 °C for 10 and 5 surfactant wt %, respectively, at fixed WOR = 40. This difference is mainly due to the surfactant amount in the mixture, for all the curves and electrolyte concentrations (not shown here, data as a whole show similar results). However, no evidence of the role of both electrolyte and WOR, on relative variation of the size of the microemulsion zone, was brought out. It remains consistent with the link that may exist, between $\Delta T_{\mu e}$ and the surfactant concentration at the oil/water interface: the cycling temperature process forces the interfacial concentration of surfactant to increase. The thermal cycles act on the surfactants, forcing them to migrate to the interface, where they reach a thermodynamically more stable state. The latter are trapped, overconcentrated, and therefore generate an increase of the global water/oil interfacial area. As a result, the microemulsion stability is enhanced, the ability to form the macroemulsions gradually decreases, and the transitional region becomes larger.

These observations appear novel and original, and such an effect, enlarging the microemulsion region, may prove to be closely related to the phenomena governing the recent formulation approaches using temperature cycling technology previously introduced.[54−59] Typically, temperature cycling is performed around the PIT of a ternary {water; nonionic surfactant; oil} system at given and particular compositions; afterward the system is broken up with a sudden water dilution or even with a rapid cooling and then a suspension of nanometer-scale droplets, capsules, or particles is generated. In these formulations the temperature treatment is necessary to create the nanometer template, and it is coherent with the assumptions discussed above, which correlate fineness of the microemulsion network and T-cycling. The bicontinuous network is more and more structured along the cycling process, and its fineness is gradually improved, progressively giving rise to the nanometer template generation. Finally, the correlation is achieved comparing (i) on the one hand, that the main condition to perform these formulations of nanosuspension using cycling technology is the use of a relatively large amount of surfactant, typically[55,56] between 10 and 40 wt %, and on the other hand (ii) the fact brought out in this study, of making the surfactant amount the main factor which induces this effect of microemulsion zone enlarging.

Conclusions

We have brought out new phenomena concerning emulsion phase inversion, and induced by a thermal cycling treatment. This study was focused on the follow-up of the macroscopic emulsion structure under a process of temperature scan through the phase inversion zone. The location of the emulsion inversion (as T_{Rise}) and the size of the transitional region between macroemulsions (as $\Delta T_{\mu e}$) were chosen as macroscopic parameters, which reflect microscopic effects due to molecular and intermolecular organization. Mainly two irreversible phenomena induced by temperature cycling were reported: the salting-out effect which creates a shift of the emulsion inversion toward lower temperatures, and an effect which enlarges the transitional microemulsion zone. These two effects are proved to be independent since they are generated by distinct composition and/or formulation parameters. Indeed, the decrease of T_{Rise} is strongly linked to the electrolyte concentration and to the WOR, whereas the rise of $\Delta T_{\mu e}$ is linked to the surfactant amount. Two approaches to explain these results are presented as the transposition of the well-described volumic theories to the water/oil interface. They are both revealed to suitably fit the experimental results, establishing an interesting parallel between the volumic and interfacial approaches. Finally, a novel insight into the emulsion phase inversion and also into the role of temperature cycling was proposed in this study; it may provide new ideas about the phenomena governing the formulation processes using cycling technology, and even about the PIT method.

Acknowledgment. We wish to express our thanks to Mr. César Pasquier for the care he took in carrying out the experiments.

References and Notes

(1) Collins, K. D.; Washabaugh, M. W. *Q. Rev. Biophys.* **1985**, *18*, 323.
(2) Kavanau, J. L. *Water and Solute-Water Interactions*; Holden-Day: San Francisco, CA, 1964.
(3) Kjellander, R. J. *J. Chem. Soc., Faraday Trans. 2* **1982**, *78*, 2025.
(4) Nilsson, P. G.; Wennerstrom, H.; Lindman, B. *J. Phys. Chem.* **1983**, *87*, 1377.
(5) Nilsson, P. G.; Lindman, B. *J. Phys. Chem.* **1983**, *87*, 4756.
(6) Jonsson, B.; Nilsson, P. G.; Lindmann, B.; Guldbrand, L.; Wennerstrom, H. *Surfactants in Solution*; Plenum: New York, 1984; Vol. 1.
(7) Funari, S. S.; Holmes, M. C.; Tiddy, G. J. T. *J. Phys. Chem.* **1994**, *98*, 3015.
(8) Romsted, L. S.; Yao, J. *Langmuir* **1996**, *12*, 2425.
(9) Hsiao, L.; Dunning, H. N.; Lorenz, P. B. *J. Phys. Chem.* **1956**, *60*, 657.
(10) Becher, P. *J. Colloid Interface Sci.* **1956**, *17*, 325.
(11) Schick, M. *J. Colloid Interface Sci.* **1962**, *17*, 801.
(12) Schick, M. J.; Atlas, S. M.; Eirich, F. R. *J. Phys. Chem.* **1962**, *66*, 1326.
(13) Schick, M. J. *J. Phys. Chem.* **1964**, *68*, 3585.
(14) Arai, H. *J. Colloid Interface Sci.* **1967**, *23*, 348.
(15) Malik, W. U.; Saleem, S. M. *J. Am. Oil Chem. Soc.* **1968**, *45*, 670.
(16) Malik, W. U.; Jhamb, O. P. *Kolloid Z. Z. Polym.* **1970**, *242*, 1209.
(17) Mukerjee, P. *J. Phys. Chem.* **1965**, *69*, 4038.
(18) Ray, A.; Nemethy, G. *J. Am. Chem. Soc.* **1971**, *93*, 6787.
(19) Schott, H.; Han, S. K. *J. Pharm. Sci.* **1976**, *65*, 975.
(20) Maclay, W. M. *J. Colloid Interface Sci.* **1956**, *11*, 272.
(21) Saito, H.; K., S. *J. Colloid Interface Sci.* **1967**, *24*, 10.
(22) Doren, A.; Goldfarb, J. *J. Colloid Interface Sci.* **1970**, *32*, 67.
(23) Shinoda, K.; Takeda, H. *J. Colloid Interface Sci.* **1970**, *32*, 642.
(24) Schott, H. *J. Colloid Interface Sci.* **1973**, *43*, 150.
(25) Schott, H. *J. Colloid Interface Sci.* **1998**, *205*, 496.
(26) Deguchi, K.; Meguro, K. *J. Colloid Interface Sci.* **1975**, *50*, 223.
(27) Marszall, L. *Tenside Deterg.* **1981**, *18*, 25.
(28) Valaulikar, B. S.; Manohar, C. *J. Colloid Interface Sci.* **1985**, *108*, 403.
(29) Gu, T.; Ma, C. *J. Colloid Interface Sci.* **1989**, *127*, 586.
(30) Sadaghiana, A. S.; Khan, A. *J. Colloid Interface Sci.* **1991**, *144*, 191.
(31) Schott, H. *J. Colloid Interface Sci.* **1995**, *173*, 265.
(32) Schott, H.; Han, S. K. *J. Pharm. Sci.* **1976**, *65*, 979.
(33) Schott, H.; Han, S. K. *J. Pharm. Sci.* **1975**, *64*, 658.
(34) Schott, H.; Royce, A. E. *J. Pharm. Sci.* **1984**, *73*, 793.
(35) Schott, H.; Royce, A. E.; Han, S. K. *J. Colloid Interface Sci.* **1984**, *98*, 196.
(36) Schott, H. *Colloids Surf., A* **2001**, *186*, 129.
(37) Schott, H. *J. Colloid Interface Sci.* **1997**, *189*, 117.
(38) Goldstein, R. E. *J. Phys. Chem.* **1984**, *80*, 5340.
(39) Wartewig, S.; Alig, I.; Hergeth, W. D.; Lange, J.; Lochmann, I.; Scherzed, T. *J. Mol. Struct.* **1990**, *219*, 365.
(40) Karlstrom, G. *J. Phys. Chem.* **1985**, *89*, 4962.
(41) Karlstrom, G.; Lindman, B. *Organized solutions*; Marcel Dekker: New York, 1992.
(42) Blandamer, M. J.; Powell, M. F.; Fox, A.; Stafford, J. L. *Makromol. Chem.* **1969**, *124*, 222.
(43) Kjellander, R. J.; Florin, E. *J. Chem. Soc., Faraday Trans. 1* **1981**, *77*, 2053.
(44) Hagler, A. T.; Scheraga, H. A.; Nemethy, G. *J. Phys. Chem.* **1972**, *76*, 3229.
(45) Schott, H. *J. Pharm. Sci.* **1980**, *69*, 369.
(46) Hołyst, R.; Staniszewski, K.; Patkowski, A.; Gapiński, J. *J. Phys. Chem. B* **2005**, *109*, 8533.
(47) Graca, M.; Wieczorek, S. A.; Hołyst, R. *Macromolecules* **2002**, *35*, 7718.
(48) Graca, M.; Wieczorek, S. A.; Fiałkowski, M.; Hołyst, R. *Macromolecules* **2002**, *35*, 9117.
(49) Goel, S. K. *J. Surfactants Deterg. (AOCS)* **1998**, *2*, 213.
(50) Szymanowski, J.; Pietrzak, E.; Wisniewski, M.; Prochaska, K. *Tenside Deterg.* **1983**, *20*, 4.
(51) Salager, J. L.; Forgiarini, A.; Marquez, L.; Pena, A.; Pizzino, A.; Rodriguez, M. P.; Rondon-Gonzalez, M. *Adv. Colloid Interface Sci.* **2004**, *108*−*109*, 259.
(52) Forster, T.; Von Rybinski, W.; Wadle, A. *Adv. Colloid Interface Sci.* **1995**, *58*, 119.
(53) Morales, D.; Gutierrez, J. M.; Garcia-Celma, M. J.; Solans, C. *Langmuir* **2003**, *19*, 7196.
(54) Heurtault, B.; Saulnier, P.; Pech, B.; Proust, J. E.; Richard, J.; Benoit, J. P. Patent W001/64328, 2001.
(55) Heurtault, B.; Saulnier, P.; Pech, B.; Proust, J. E.; Benoit, J. P. *Pharm. Res.* **2002**, *19*, 875.
(56) Béduneau, A.; Saulnier, P.; Anton, N.; Hindré, F.; Passirani, C.; Rajerison, H.; Noiret, N.; Benoit, J.-P. *Pharm. Res.* **2006**, *23*, 2190.
(57) Hoarau, D.; Delmas, P.; David, S.; Roux, E.; Leroux, J. C. *Pharm. Res.* **2004**, *21*, 1783.
(58) Lamprecht, A.; Bouligand, Y.; Benoit, J. P. *J. Controlled Release* **2002**, *84*, 59.
(59) Malzert, A.; Vrignaud, S.; Saulnier, P.; Lisowski, V.; Benoit, J. P.; Rault, S. *Int. J. Pharm.* **2006**, *320*, 157.
(60) Lehnert, S.; Tarabishi, H.; Leuenberger, H. *Colloids Surf., A* **1994**, *91*, 227.
(61) Minana-Perez, M.; Gutron, C.; Zundel, C.; Anderez, J. M.; Salager, J. L. *J. Dispersion Sci. Technol.* **1999**, *20*, 893.
(62) Salager, J. L.; Loaiza-Maldonado, I.; Minana-Perez, M.; Silva, F. *J. Dispersion Sci. Technol.* **1982**, *3*, 279.
(63) Graciaa, A.; Lachaide, J.; Sayous, J. G.; Grenier, P.; Yiv, S.; Schechter, R. S.; Wade, W. H. *J. Colloid Interface Sci.* **1983**, *93*, 474.
(64) Goel, S. K. *J. Colloid Interface Sci.* **1999**, *212*, 604.
(65) Aveyard, R.; Binks, B. P.; Clark, S.; Fletcher, P. D. *J. Chem. Soc., Faraday Trans.* **1990**, *86*, 3111.
(66) Penfold, J.; Staples, E.; Tucker, I.; Thompson, L.; Thomas, R. K. *J. Colloid Interface Sci.* **2002**, *247*, 404.